

IL NUOVO CIMENTO
NOTE BREVI
DOI 10.1393/ncc/i2006-10024-0

VOL. 30 C, N. 2

Marzo-Aprile 2007

On the additional boundary condition of wind-driven ocean models on the eastern coast

F. CRISCIANI⁽¹⁾(*), F. CAVALLINI⁽²⁾ and R. MOSETTI⁽²⁾

⁽¹⁾ ISMAR-CNR, Istituto di Scienze Marine del CNR - Trieste, Italy

⁽²⁾ OGS, Istituto Nazionale di Oceanografia e di Geofisica Sperimentale - Trieste, Italy

(ricevuto il 26 Luglio 2006; approvato il 6 Maggio 2007; pubblicato online il 7 Agosto 2007)

Summary. — In the homogeneous model of the wind-driven ocean circulation, the dynamics of the basin interior is basically governed by the Sverdrup balance and the related no mass-flux condition on the eastern boundary of the basin, which we assume to be square for conceptual simplicity. In the presence of lateral diffusion of relative vorticity, the additional condition on the eastern boundary (like the conditions on the other boundaries) is not demanded on physical grounds but it is arbitrary to a large extent. Hence, certain choices of such boundary condition can produce overall solutions which are “far” from that of Sverdrup in the eastern part of the domain, without any physical reason. In the present note we show that this discrepancy can be strongly reduced if the adopted additional boundary condition has the same form as that *implicitly* satisfied by the Sverdrup solution. Unlike the common approach, a criterion is thus derived which selects a suitable partial slip boundary condition according to the specific wind-stress field which is taken into account.

PACS 92.10.Fj – Upper ocean and mixed layer processes.

PACS 92.10.Lq – Turbulence, diffusion, and mixing processes in oceanography.

1. – Introduction

In the theory of the wind-driven oceanic circulation on the basin-scale, the turbulent dissipation of vorticity, which is put in the water body by the wind-stress, is an indispensable dynamical mechanism for the maintenance of a steady circulation. Since 1950, lateral diffusion of relative vorticity has been a common constituent of the parameterization of turbulence whose adoption, in the case of a bounded fluid domain, demands additional boundary conditions (hereafter ABCs) to single out a unique model solution [1]. We stress that the actual form of the ABCs is left partially undefined so a still open question is posed by the lack of uniqueness of the ABCs: in fact several ABCs are admissible, each of them having its own kinematical meaning and influence on the

(*) E-mail: fulvio.crisciani@ts.ismar.cnr.it

model solution, but no criterion is known to select the “true” or the “best” condition according to a shared physical viewpoint. We recall the asymmetric role of the turbulent dissipation in the western and in the eastern parts of the basin: in the dynamics of the western boundary layer, turbulent dissipation has the same order of magnitude as the meridional velocity coupled with the planetary vorticity gradient thus giving rise to the westward intensification [2] while, in the remaining part of the basin, turbulent dissipation becomes almost negligible and the same meridional velocity is prevalently balanced by the wind-stress curl according to the well-known Sverdrup relation [3]. However, although turbulent dissipation plays a minor role in the eastern part of the basin, the flow is requested to satisfy a prescribed ABC also at the eastern boundary. On the other hand, whatever the ABC may be, it is *not* introduced on basic physical grounds and this is ultimately the reason of the lack of uniqueness of the ABCs.

Here, we point out a criterion for the selection of the ABC at the eastern boundary in the framework of the homogeneous model of the wind-driven circulation and, in particular, we focus our attention to the frictional regime (sect. 2). The investigation is based on the following considerations. The weak turbulent dissipation and the low inertia of this regime allow the Sverdrup solution to emerge as the dominant term of the complete solution in the interior and eastern part of the basin. Once the validity of the Sverdrup balance in such an area is recognized, the resort to *any* ABC (which is necessarily demanded, no matter how weak lateral diffusion is) seems to be questionable because of the possible discrepancy arising, in the proximity of the eastern wall, between the Sverdrup solution and the total solution. In fact, the latter depends critically on the kind of ABC which is selected at the eastern boundary while the former is quite independent of it (sect. 3). Even if nothing prevents us from conceiving solutions markedly different from that of Sverdrup in an appropriate eastern boundary layer, at the same time their lack of physical grounds should be borne in mind.

In the present note, we show that the above discrepancy can be strongly damped if the adopted ABC has the same form as one that is *implicitly* satisfied by the Sverdrup solution (sect. 4). Finally, we stress that, since the ABCs are left unaffected by non-linearity, the ABC so derived in the frictional regime still holds, as it stands, in the fully non-linear mode.

2. – Preliminaries on the homogeneous model

We shortly recall the non-dimensional version of the homogeneous model in the case of steady circulation and neglecting, for simplicity, bottom friction. The notation and the meaning of the symbols are those reported in [4].

The governing vorticity equation is

$$(2.1) \quad (\delta_I/L)^2 J(\psi, \nabla^2 \psi) + \frac{\partial \psi}{\partial x} = w_E(x, y) + (\delta_M/L)^3 \nabla^4 \psi \quad \forall (x, y) \in D,$$

where D is the square fluid domain

$$(2.2) \quad D = [0 \leq x \leq 1] \times [0 \leq y \leq 1]$$

of a certain β -plane. The no mass-flux condition holds throughout the boundary ∂D of D , that is

$$(2.3) \quad \psi = 0 \quad \forall (x, y) \in \partial D.$$

In particular, δ_I/L is the non-dimensional width of the inertial boundary layer, while δ_M/L is the non-dimensional width of the frictional boundary layer. In the frictional regime we have

$$(2.4) \quad \delta_I \ll \delta_M,$$

and the order of magnitude of the length δ_I cannot be realistically smaller than $O(10^4)$ in SI units.

It is known that the non-dimensional $O(1)$ vertical velocity w_E induced by the Ekman pumping matches the wind-stress curl on the sea surface with the geostrophic flow. Actually, $w_E(x, y)$ is the result of a space smoothing of the true wind-stress curl which preserves only its slowly varying part. This is the reason why $w_E(x, y)$ is usually taken as some simple analytical function of x and y , mostly sinusoidal in y . Widely used expressions of $w_E(x, y)$ for an idealized subtropical gyre are

$$(2.5) \quad w_E(x, y) = -\sin(\pi y),$$

or

$$(2.6) \quad w_E(x, y) = -\sin(\pi x) \sin(\pi y).$$

The composite form

$$(2.7) \quad w_E(x, y) = -(\alpha \sin(\pi x) + 1 - \alpha) \sin(\pi y), \quad (0 \leq \alpha \leq 1),$$

which coincides with (2.5) and (2.6) for $\alpha = 0$ and $\alpha = 1$, respectively, will also be used in the subsequent discussion.

The crucial point is that the fourth-order derivatives of $\nabla^4 \psi$ raise the order of the differential equation (2.1) and, in order to single out a unique model solution, they demand additional boundary conditions which are the subject of the present investigation.

Because of (2.4), the strictly linear version of (2.1) takes the form

$$(2.8) \quad \frac{\partial \psi}{\partial x} = w_E(x, y) + (\delta_M/L)^3 \nabla^4 \psi,$$

where $(\delta_M/L)^3 = O(10^{-3})$, at least, if $L = O(10^6)$ in SI units.

In the ocean interior (subscript I), both $(\delta_I/L)^2$ and $(\delta_M/L)^3$ are much smaller than unity, so in (2.1) the $O(1)$ meridional velocity equilibrates along the $O(1)$ wind-stress curl, thus yielding the Sverdrup balance

$$(2.9) \quad \frac{\partial \psi_I}{\partial x} = w_E(x, y).$$

The interior stream function $\psi_I(x, y)$, satisfying (2.9), is subject to the no mass-flux condition at the eastern boundary, *i.e.*

$$(2.10) \quad \psi_I(1, y) = 0,$$

so, from (2.9) and (2.10) the Sverdrup solution

$$(2.11) \quad \psi_I = - \int_x^1 w_E(x', y) dx'$$

follows. We stress again that, in the frictional regime, the Sverdrup solution (2.11) is recognized to be the dominant part of the complete solution from the interior as far as the eastern wall. In particular, the meridional velocity $v_I(1, y)$ along the eastern boundary is fully determined by the forcing w_E evaluated at the same place, *i.e.*

$$(2.12) \quad v_I(1, y) \equiv \left[\frac{\partial \psi_I}{\partial x} \right]_{x=1} = w_E(1, y).$$

We also recall the energy equation coming from (2.1) and (2.3), which we shall use in sect. 4 to check the physical consistency of the boundary condition under scrutiny. Multiplication of (2.1) by $-\psi$ and the subsequent integration on D with the aid of (2.3) and the repeated use of the divergence theorem yields the equation (see [4] for details)

$$(2.13) \quad \frac{dK}{dt} = - \int_D \psi w_E dx dy + (\delta_M/L)^3 \oint_{\partial D} \nabla^2 \psi \vec{\nabla} \psi \cdot \hat{n} ds - (\delta_M/L)^3 \int_D (\nabla^2 \psi)^2 dx dy,$$

where $K = (1/2) \int_D |\vec{\nabla} \psi|^2 dx dy$ is the integrated kinetic energy of the system, the first integral on the r.h.s. of (2.13) is the time rate of change of the energy source due to the wind forcing and it is expressed as a pressure work. The circuit integral on the r.h.s. of (2.13), where \hat{n} is the unit vector locally normal to ∂D and ds is the differential arclength along ∂D , is the problematic part of this equation in the case in which it is positive. In fact, if the forcing is turned off from a given time on, we expect the kinetic energy to decrease to zero because of its erosion due to the lateral diffusion of relative vorticity. This situation is favoured by the negative definite term $-(\delta_M/L)^3 \int_D (\nabla^2 \psi)^2 dx dy$ of (2.13), but a positive contribution from the circuit integral might reverse the sign of the whole expression $-(\delta_M/L)^3 \int_D (\nabla^2 \psi)^2 dx dy + (\delta_M/L)^3 \oint_{\partial D} \nabla^2 \psi \vec{\nabla} \psi \cdot \hat{n} ds$ and hence the sign of the time rate of change of the kinetic energy. Indeed, the circuit integral is trivially zero if the no-slip (*i.e.* $\hat{n} \cdot \vec{\nabla} \psi = 0$ on ∂D) or the free-slip (*i.e.* $\nabla^2 \psi = 0$ on ∂D) conditions are applied; but its sign is not obvious, for instance, if a partial slip condition is considered. For future purposes, we report the contribution, say E , to $\oint_{C_D} \nabla^2 \psi \vec{\nabla} \psi \cdot \hat{n} ds$ coming from the eastern boundary: with reference to (2.2), it is given by

$$(2.14) \quad E = \int_0^1 \left[\frac{\partial^2 \psi}{\partial x^2} \frac{\partial \psi}{\partial x} \right]_{x=1} dy.$$

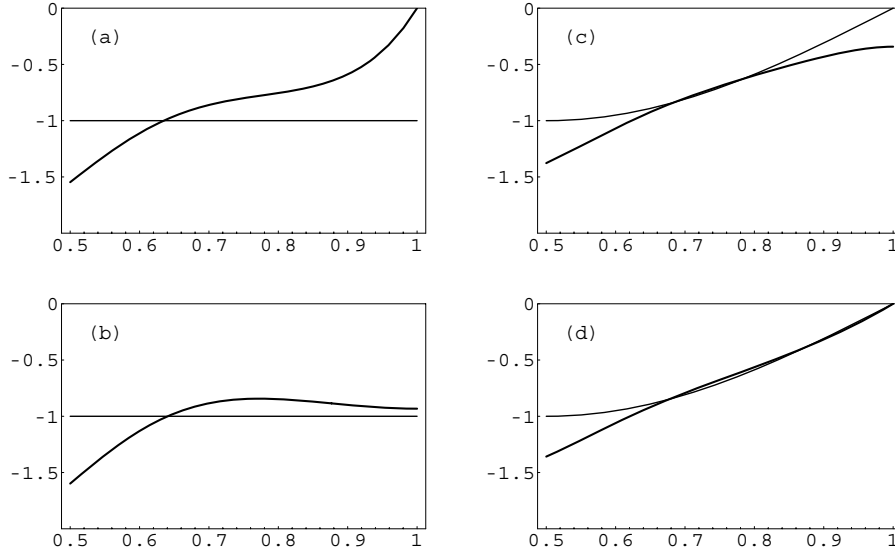


Fig. 1. – Mid-latitude meridional velocity v (thick line) and Sverdrup meridional velocity v_I (thin line) from the central longitude of the basin to the eastern boundary. Panels (a) and (b) refer to forcing (2.5), while panels (c) and (d) refer to forcing (2.6). The figure points out the discrepancy between v and v_I whose amount depends on the choice of the ABC which is applied on the eastern boundary ($x = 1$) to evaluate v .

3. – Illustrative examples

To illustrate the unphysical discrepancy that can arise between the Sverdrup solution and the complete solution in the proximity of the eastern wall (in $x = 1$), we point out what happens in two cases, using (2.2), (2.3), (2.8) and setting $(\delta_M/L)^3 = 10^{-3}$. We anticipate that the choice of the free-slip condition on the western boundary is purely conventional in all the subsequent examples, sect. 4 included.

First case: forcing is (2.5).

- a) The ABCs are no slip on the eastern boundary and free slip on the other boundaries. The mid-latitude meridional velocity $v(x, 1/2)$ is reported in panel (a) of fig. 1 (thick line) starting from the central longitude of the basin to the eastern boundary. The thin line represents the constant meridional velocity $v_I(x, 1/2)$ evaluated from the Sverdrup solution (recall (2.12)). Note that, unlike $v(x, 1/2)$, $v_I(x, 1/2)$ implicitly satisfies the free-slip ABC in $x = 1$. While the departure of $v(x, 1/2)$ from $v_I(x, 1/2)$ far from the eastern boundary is a typical consequence of the beta-plane dynamics, the departure of $v(x, 1/2)$ from $v_I(x, 1/2)$ near the eastern wall is entirely due to the assumed no-slip ABC.
- b) The free-slip ABC is applied also along the eastern boundary. The result is that depicted in panel (b) of fig. 1. While the situation is the same as before in the interior, the tendency of $v(x, 1/2)$ to follow $v_I(x, 1/2)$ in the easternmost part of the basin is evident and it is explained simply by the fact that both $v(x, 1/2)$ and $v_I(x, 1/2)$ now satisfy the same ABC in $x = 1$.

Second case: the forcing is (2.6).

- c) The ABCs are free slip on all the boundaries. The resulting meridional velocities $v(x, 1/2)$ (thick line) and $v_I(x, 1/2)$ (thin line) are shown in panel (c) of fig. 1. Note that, unlike $v(x, 1/2)$, here $v_I(x, 1/2)$ implicitly satisfies the no-slip ABC in $x = 1$, and this is the reason why a net departure of $v(x, 1/2)$ from $v_I(x, 1/2)$ is observed for longitudes close to $x = 1$.
- d) Free slip with the no-slip ABC in $x = 1$. Velocity $v(x, 1/2)$ goes as in panel (d) of fig. 1 and a full coincidence of $v(x, 1/2)$ with $v_I(x, 1/2)$ is established. As in the first case, the further departure of $v(x, 1/2)$ from $v_I(x, 1/2)$ in the interior is explained by the beta-effect and it is not heavily affected by the special ABC which is taken into account.

4. – Additional conditions at the eastern boundary

The above examples give us the hint to derive the boundary conditions that are consistent with the Sverdrup solution starting from the related balance.

From (2.9) and the second x -derivative of the same equation, both evaluated at $x = 1$, we trivially obtain $[\frac{\partial \psi_I}{\partial x}]_{x=1} = w_E(1, y)$ and $[\frac{\partial^2 \psi_I}{\partial x^2}]_{x=1} = [\frac{\partial w_E}{\partial x}]_{x=1}$ respectively, whence the identity

$$(4.1) \quad \left[\frac{\partial w_E}{\partial x} \right]_{x=1} \left[\frac{\partial \psi_I}{\partial x} \right]_{x=1} - w_E(1, y) \left[\frac{\partial^2 \psi_I}{\partial x^2} \right]_{x=1} = 0$$

follows. Equation (4.1) has the form of a boundary condition for ψ_I in $x = 1$, which is implicitly verified by ψ_I . Now, if the total stream function ψ satisfies the ABC

$$(4.2) \quad \left[\frac{\partial w_E}{\partial x} \right]_{x=1} \left[\frac{\partial \psi}{\partial x} \right]_{x=1} - w_E(1, y) \left[\frac{\partial^2 \psi}{\partial x^2} \right]_{x=1} = 0$$

which is nothing but (4.1) referred to ψ , then we expect ψ to be very close to ψ_I in the proximity of the eastern boundary. In this way the ABC in the form (4.2) arranges the complete solution in a configuration that, near the eastern boundary, is not “too far” from that of Sverdrup. Equation (4.2) expresses the criterion proposed in the present note to select the ABC on the eastern coast of the basin.

The cases pointed out in sect. 3 are easily found again using (4.2). In fact, if the forcing (2.5) is taken into account, then $\partial w_E / \partial x \equiv 0$ and $w_E(1, y) \neq 0$. Hence (4.2) implies $[\frac{\partial^2 \psi}{\partial x^2}]_{x=1} = 0$, that is the free-slip condition appearing in panel (b) of fig. 1. On the other hand, if the forcing (2.6) is taken into account, then $w_E(1, y) = 0$ and $[\frac{\partial w_E}{\partial x}]_{x=1} = -\pi \sin(\pi y) \neq 0$. Hence (4.2) implies $[\frac{\partial \psi}{\partial x}]_{x=1} = 0$, that is the no-slip condition appearing in panel (d) of fig. 1.

Moreover, (2.14) gives $E = 0$ in both cases so the above ABCs do not contribute to the energy of the flow.

If the forcing (2.7) is taken into account with $0 < \alpha < 1$, the ABC (4.2) is a partial slip, *i.e.*

$$(4.3) \quad \pi \alpha \left[\frac{\partial \psi}{\partial x} \right]_{x=1} - (\alpha - 1) \left[\frac{\partial^2 \psi}{\partial x^2} \right]_{x=1} = 0$$

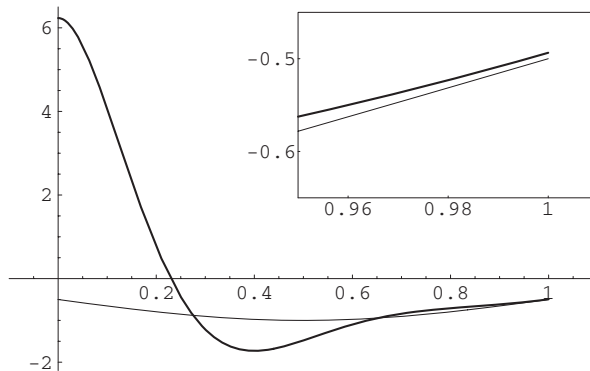


Fig. 2. – Mid-latitude meridional velocity v (thick line) and Sverdrup meridional velocity v_I (thin line) given by (4.6). Velocity v satisfies the ABC $\pi v(1, \pi/2) + [\frac{\partial v}{\partial x}]_{x=1} = 0$, that is (4.5) which is a special case of (4.2). The plot shows the marked damping of the difference $v - v_I$ in the eastern part of the fluid domain. The zoom in the internal panel details this difference for longitudes very close to $x = 1$.

and (2.14) yields

$$(4.4) \quad E = \frac{\alpha - 1}{\pi\alpha} \int_0^1 \left(\left[\frac{\partial^2 \psi}{\partial x^2} \right]_{x=1} \right)^2 dy.$$

The r.h.s. of (4.4) shows that, unlike the previous cases (2.5) and (2.6), case (2.7) implies $E < 0$: thus also in this case the boundary does not generate energy and therefore (4.3) is physically consistent.

Example. The forcing is (2.7) with $\alpha = 1/2$ and the ABCs are (4.3) on the eastern boundary, that is

$$(4.5) \quad \pi \left[\frac{\partial \psi}{\partial x} \right]_{x=1} + \left[\frac{\partial^2 \psi}{\partial x^2} \right]_{x=1} = 0,$$

and free slip on the other boundaries. The mid-latitude meridional velocity $v(x, 1/2)$ resulting from the model in the full longitudinal interval is reported in fig. 2 (thick line). The thin line represents the meridional velocity

$$(4.6) \quad v_I(x, 1/2) = -(1 + \sin(\pi x))/2$$

evaluated from the Sverdrup solution. In the internal panel a zoom is depicted to detail the behaviour of the above velocities in the proximity of the eastern wall. They differ for a relatively small amount and also the relative vorticities $[\frac{\partial v}{\partial x}]_{x=1}$, $[\frac{\partial v_I}{\partial x}]_{x=1}$ are almost the same. This result proves further on the validity of criterion (4.2) to obtain a model solution close to that of Sverdrup in the eastern region of the fluid domain.

5. – Outline and concluding remarks

1) In the homogeneous model, the dynamics of the basin scale circulation in the ocean interior is basically funded on the Sverdrup balance (2.9) and the related no mass-flux

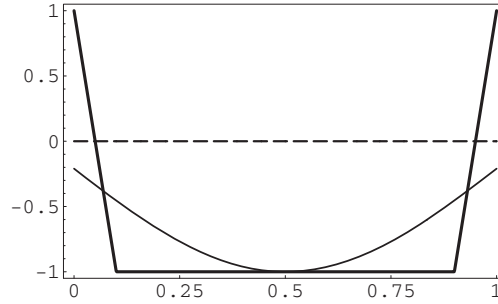


Fig. 3. – Plot of the assumed meridional velocity (5.3) (thick graph) and its best fit from ansatz (5.4), (5.5) for $\lambda/L = 0.1$. For convenience, the zero value is also shown (broken line).

boundary condition (2.10). In the presence of lateral diffusion of relative vorticity, the application of the ABC (4.2) produces a solution close to that of Sverdrup in the eastern part of the domain, without any correction *ad hoc* which would be lacking of physical grounds. Unlike the common approach, the so obtained ABC does depend on the slowly varying part of the wind-stress field of the considered model.

2) Apart from the idealized forcing fields (2.5), (2.6) and (2.7), the substitution of (4.2) into (2.14) gives

$$(5.1) \quad E = \int_0^1 \left[\left(\frac{\partial \psi}{\partial x} \right)^2 \frac{\partial w_E}{\partial x} / w_E \right]_{x=1} dy,$$

or

$$(5.2) \quad E = \int_0^1 \left[\left(\frac{\partial^2 \psi}{\partial x^2} \right)^2 w_E / \frac{\partial w_E}{\partial x} \right]_{x=1} dy.$$

Equations (5.1) and (5.2) show that the ratio $[\frac{\partial w_E}{\partial x} / w_E]_{x=1}$ or its reciprocal are crucial to establish whether $E \leq 0$ or not and, in this latter case, the use of the partial slip boundary condition derived from (4.2) could be problematic. This aspect can be hardly resolved only by means of theoretical considerations and the inspection of realistic configurations are in order. For instance, the map of the yearly averaged wind-stress curl of the Atlantic ocean in the area of the subtropical gyre [5] exhibits, close to the eastern coastline, positive values of the observed $\partial w_E / \partial x$ but, at the same time, also the observed w_E is, here and there, positive along the eastern coastline. Nevertheless, this behaviour takes place on a relatively small length scale λ while, in the remaining area of the basin interior, w_E is strictly negative. Therefore, the space smoothing of the actual wind-stress curl carried out on the basin scale $L \gg \lambda$ makes w_E everywhere negative and hence $E < 0$ follows. To clarify this point, let us consider the following situation depicted in fig. 3:

$$(5.3) \quad w_E(\text{observed}) \approx \begin{cases} 1 - 2x/\Lambda & \text{for } 0 \leq x \leq \Lambda \\ -1 & \text{for } \Lambda < x < 1 - \Lambda \\ 1 + 2(x - 1)/\Lambda & \text{for } 1 - \Lambda \leq x \leq 1 \end{cases} \quad (\Lambda = \lambda/L)$$

is best fitted in the class of functions (cf. (2.7))

$$(5.4) \quad w_E(x) = -\alpha \sin(\pi x) - 1 + \alpha,$$

by choosing

$$(5.5) \quad \alpha = \left(2\Lambda + \frac{4}{\pi} \left(\frac{\sin(\pi\Lambda)}{\pi\Lambda} - 1 \right) \right) \left(\frac{3}{2} - \frac{4}{\pi} \right)^{-1} \quad (\Lambda = \lambda/L).$$

Equation (5.5) implies that $\alpha < 1$ for $0 < \Lambda < 0.13$, and (4.4) yields $E < 0$ in this interval.

3) We go back again to (4.2) which, using (2.9), can be written as

$$\left[\frac{\partial^2 \psi_I}{\partial x^2} \frac{\partial \psi}{\partial x} - \frac{\partial \psi_I}{\partial x} \frac{\partial^2 \psi}{\partial x^2} \right]_{x=1} = 0.$$

The latter equation, in turn, implies

$$(5.6) \quad \left[\frac{\partial \psi}{\partial x} \right]_{x=1} = K(y) \left[\frac{\partial \psi_I}{\partial x} \right]_{x=1}.$$

Evaluation of (2.8) in $x = 1$ with the aid of (5.6) yields

$$(5.7) \quad (K(y) - 1) \left[\frac{\partial \psi_I}{\partial x} \right]_{x=1} = (\delta_M/L)^3 [\nabla^4 \psi]_{x=1},$$

where, in general,

$$(5.8) \quad (\delta_M/L)^3 [\nabla^4 \psi]_{x=1} = O((\delta_M/L)^3).$$

Now, while (5.6) trivially implies $[\frac{\partial \psi_I}{\partial x}]_{x=1} = 0 \Rightarrow [\frac{\partial \psi}{\partial x}]_{x=1} = 0$ (this is a known result), if

$$(5.9) \quad \left[\frac{\partial \psi_I}{\partial x} \right]_{x=1} = O(1),$$

the l.h.s. of (5.7) is $O((\delta_M/L)^3)$ as the r.h.s. of the same equation (recall (5.8)) provided that $K(y) - 1 = O((\delta_M/L)^3)$, that is $K(y) = O(1)$. In this case (5.6) yields

$$(5.10) \quad \left[\frac{\partial \psi}{\partial x} \right]_{x=1} = O \left(\left[\frac{\partial \psi_I}{\partial x} \right]_{x=1} \right).$$

The estimate (5.10) results both in panel (b) of fig. 1 (where $v \approx v_I = -1$) and in fig. 2 (where $v \approx v_I = -1/2$).

4) Finally, we remark that criterion (4.2) suffers from two limitations. First, it cannot work if both $w_E(1, y)$ and $[\frac{\partial w_E}{\partial x}]_{x=1}$ are zero. However this eventuality is rather special and not supported by observations. Moreover, it seems to be never taken into account in the literature. Second, lateral diffusion of relative vorticity can be present also in unsteady motions, not contemplated by (4.2), for instance in the decay of Rossby waves

included between a couple of meridional boundaries. But in the latter case the related dynamics makes rise to a quite different phenomenology, which goes beyond the scope of the present note and involves prevalingly the formation of the western boundary layer rather than the eastern one [6, 7].

REFERENCES

- [1] MUNK W. H., *J. Meteorol.*, **7** (1950) 79 (historical paper).
- [2] STOMMEL H., *Trans. Am. Geophys. Union*, **29** (1948) 202 (historical paper).
- [3] SVERDRUP H. U., *Proc. Natl. Acad. Sci., U.S.A.*, **33** (1947) 318 (historical paper).
- [4] PEDLOSKY J., *Ocean Circulation Theory* (Springer-Verlag) 1996, Chapt. 2.
- [5] LINDAU R., *Climate Atlas of the Atlantic Ocean* (Springer-Verlag) 2001, p. 476.
- [6] PEDLOSKY J., *J. Mar. Res.*, **23** (1965) 207.
- [7] PEDLOSKY J., *Geophysical Fluid Dynamics* (Springer-Verlag) 1987.